Title

Five-S-isotope evidence of two distinct mass-independent sulfur isotope effects and implications for the modern and Archean atmospheres

Journal

Proceedings of the National Academy of Sciences of the United States of America, 115(34)

ISSN

0027-8424

Authors

Lin, Mang
Zhang, Xiaolin
Li, Menghan
et al.

Publication Date

2018-08-21

DOI

10.1073/pnas.1803420115

Peer reviewed

Five-S-isotope evidence of two distinct mass-independent sulfur isotope effects and implications for the modern and Archean atmospheres

Mang Lin[a,1,2], Xiaolin Zhang[b], Menghan Li[b], Yilun Xu[b], Zhisheng Zhang[c], Jun Tao[c], Binbin Su[d], Lanzhong Liu[d], Yanan Shen[b,1], and Mark H. Thiemens[a,1]

[a]Department of Chemistry and Biochemistry, University of California, San Diego, La Jolla, CA 92093; [b]School of Earth and Space Sciences, University of Science and Technology of China, Hefei 230026, China; [c]South China Institute of Environmental Sciences, Ministry of Environmental Protection of China, Guangzhou 510655, China; and [d]National Atmospheric Background Monitoring Station in Wuyi Mountain of Fujian Province, Wuyishan 354300, China

Edited by Thure E. Cerling, University of Utah, Salt Lake City, UT, and approved July 2, 2018 (received for review February 27, 2018)

The signature of mass-independent fractionation of quadruple sulfur stable isotopes (S-MIF) in Archean rocks, ice cores, and Martian meteorites provides a unique probe of the oxygen and sulfur cycles in the terrestrial and Martian paleoatmospheres. Its mechanistic origin, however, contains some uncertainties. Even for the modern atmosphere, the primary mechanism responsible for the S-MIF observed in nearly all tropospheric sulfates has not been identified. Here we present high-sensitivity measurements of a fifth sulfur isotope, stratospherically produced radiosulfur, along with all four stable sulfur isotopes in the same sulfate aerosols and a suite of chemical species to define sources and mechanisms on a field observational basis. The five-sulfur-isotope and multiple chemical species analysis approach provides strong evidence that S-MIF signatures in tropospheric sulfates are concomitantly affected by two distinct processes: an altitude-dependent positive ^{33}S anomaly, likely linked to stratospheric SO_2 photolysis, and a negative ^{36}S anomaly mainly associated with combustion. Our quadruple stable sulfur isotopic measurements in varying coal samples (formed in the Carboniferous, Permian, and Triassic periods) and in SO_2 emitted from combustion display normal ^{33}S and ^{36}S, indicating that the observed negative ^{36}S anomalies originate from a previously unknown S-MIF mechanism during combustion (likely recombination reactions) instead of coal itself. The basic chemical physics of S-MIF in both photolytic and thermal reactions and their interplay, which were not explored together in the past, may be another ingredient for providing deeper understanding of the evolution of Earth's atmosphere and life's origin.

cosmogenic sulfur-35 | stable sulfur isotope anomalies | sulfate aerosols | combustion | recombination reactions

As the tenth most abundant element in the universe, sulfur occurs as stable (^{32}S, ^{33}S, ^{34}S, and ^{36}S) and radioactive isotopes (e.g., ^{35}S and ^{38}S). The signature of mass-independent fractionation of quadruple sulfur stable isotopes [S-MIF or sulfur isotopic anomaly, quantified by $\Delta^{33}S = \delta^{33}S - [(1 + \delta^{34}S)^{0.515} - 1]$ and $\Delta^{36}S = \delta^{36}S - [(1 + \delta^{34}S)^{1.9} - 1]$ and traditionally expressed as per mil] observed in Archean (~4 Ga to ~2.5 Ga) sediments has been interpreted as a proxy of the origin and evolution of atmospheric oxygen and early life on Earth (1, 2). Resolving all mechanistic origins of S-MIF has been a focus of active research for more than 20 y (3). Photochemistry of sulfur-bearing gases (e.g., SO_2 and H_2S) in the short-wavelength UV region accounts for much of the Archean record and is the currently most accepted mechanism responsible for S-MIF observed on Earth (1, 2, 4), Mars (5), and possibly achondritic meteorites (6).

In modern Earth, only stratospheric sulfates are presumed to acquire S-MIF signatures, because short (<~290 nm) UV light is shielded by the stratospheric ozone layer. The presence of S-MIF in sulfates extracted from ice cores, snow pits, and ash beds is interpreted as deriving from massive volcanic eruptions with stratospheric SO_2 injection (7–9). This assumption may not always be valid, because sulfur isotopic anomalies not explicable by mass-dependent fractionation (MDF) (10) are widely found in tropospheric sulfates (11–15) (Fig. 1). Stratospheric influence on the unexpected S-MIF in tropospheric sulfates, which has been speculated about for more than 15 y (11–16), remains unquantified for lack of a measurable stratospheric tracer of the sulfate. Recently, combustion processes were also speculated on as an additional potential source for S-MIF in tropospheric sulfates (15, 16), but unambiguous evidence is absent because (*i*) the direct relationship between combustion and S-MIF signature in ambient tropospheric aerosols is not demonstrated by combustion tracer measurements and (*ii*) multiple sulfur isotopic compositions in fuels for combustion have not been reported. Without a complete understanding of the origin of S-MIF in modern atmospheric sulfates, interpretation of S-MIF signals preserved in cryospheric, geological, and meteoritic samples possesses embedded uncertainties.

In this study, the high-sensitivity measurement (17, 18) of a fifth sulfur isotope, ^{35}S (half-life: ~87 d), casts light on the exploration of the origin of S-MIF in atmospheric sulfates on a field observational basis. Cosmogenic ^{35}S is the only radioactive sulfur isotope existing

Significance

Anomalous sulfur isotopic compositions preserved in sedimentary rocks older than ~2.5 billion years have been widely interpreted as the products of UV photolysis of sulfur dioxide in an anoxic atmosphere and used to track the history of primitive Earth and evolution of early life. In this study, we present strong observational evidence that there is an additional process that produces similar anomalous sulfur isotope signatures. This previously unknown origin not only offers a tool for quantifying the present-day atmospheric sulfur budget and evaluating its influences on climate and public health but also implies that anomalous sulfur isotopic compositions in some of the oldest rocks on Earth might have been produced in a way different from that previously thought.

Author contributions: M. Lin, Y.S., and M.H.T. designed research; M. Lin, X.Z., M. Li, Y.X., Z.Z., J.T., B.S., L.L., and Y.S. performed research; M. Lin, Y.S., and M.H.T. contributed new reagents/analytic tools; M. Lin analyzed data; and M. Lin, Y.S., and M.H.T. wrote the paper.

The authors declare no conflict of interest.

This article is a PNAS Direct Submission.

[1]To whom correspondence may be addressed. Email: manglin.ucsd@gmail.com, yashen@ustc.edu.cn, or mthiemens@ucsd.edu.

[2]Present addresses: School of Materials and Chemical Technology, Tokyo Institute of Technology, 226-8502 Yokohama, Japan; and Earth-Life Science Institute, Tokyo Institute of Technology, 152-8550 Tokyo, Japan.

This article contains supporting information online at www.pnas.org/lookup/suppl/doi:10.1073/pnas.1803420115/-/DCSupplemental.

Published online August 6, 2018.

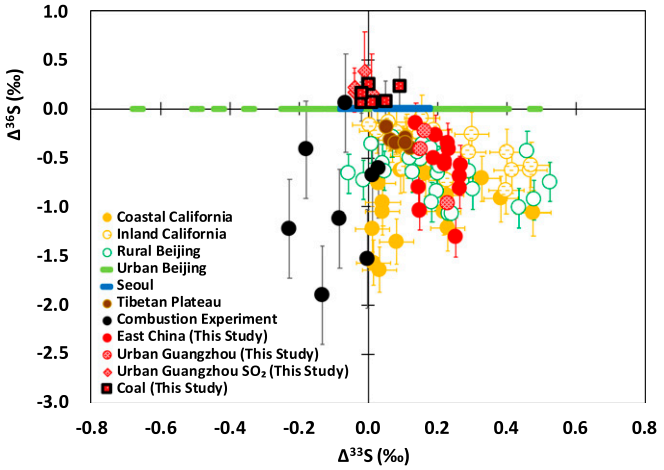

Fig. 1. Quadruple stable sulfur isotopic compositions in modern tropospheric sulfates, SO_2, and coal. Atmospheric samples were collected from a background site at East China (the Mount Wuyi Station; this study), the third largest megacity in China (Guangzhou; this study), coastal California (11), inland California (11), rural Beijing (12), urban Beijing (13), Seoul (14), and Tibetan Plateau (15). Note that $\Delta^{36}S$ data for urban Beijing (13) and Seoul (14) are not available, and therefore $\Delta^{33}S$ data are shown on the *x* axis as bars. Chromium-reducible sulfur in coal (this study) and primary sulfates emitted from a chamber combustion experiment (29) are also shown. Error bars stand for 1 SD.

in nature with a half-life of ideal age to track atmospheric processes (17). It is exclusively produced in the higher atmosphere by the spallogenic bombardment of ^{40}Ar by high-energy cosmic rays. The ability of ^{35}S to serve as a sensitive and unambiguous tracer in identifying sulfate aerosols originating from the higher atmosphere was recently demonstrated (19) and has been utilized in understanding sulfate formation pathways at different altitudes (20). Here we report all five (four stable and one radioactive) sulfur isotopes' and all three stable oxygen isotopes' (^{16}O, ^{17}O, and ^{18}O) composition in sulfate along with other inorganic and organic compounds in the same aerosols collected at a midlatitude remote mountain site located in East Asia (*Materials and Methods* and *SI Appendix*, Fig. S1) to trace the origins of S-MIF signatures.

Quadruple Sulfur Isotope Composition in Sulfate Aerosols, SO_2, and Coal

All sulfate aerosols measured in this study possess nonzero $\Delta^{33}S$ and $\Delta^{36}S$ values (Fig. 1), consistent with previous measurements (11–15). Because coal burning accounts for ∼95% of sulfur emissions in China (21) and it has been speculated that sulfur isotopic anomalies of present-day aerosols might originate from coal (12), we first measured quadruple stable sulfur isotopes in various representative Chinese coal samples [formed in the Carboniferous, Permian, and Triassic periods, in which 90% of the total recoverable coal reserves across China were formed (22)] and ambient SO_2 emitted from coal burning (*Materials and Methods*) to evaluate their contribution to nonzero $\Delta^{33}S$ and $\Delta^{36}S$ values in atmospheric sulfates. Our data indicate that sulfur isotopic compositions in coal and SO_2 are essentially normal within error, and their patterns in the $\Delta^{33}S$ vs. $\Delta^{36}S$ scatter plot notably differ from tropospheric sulfates (Fig. 1). It is therefore highly unlikely that nonzero $\Delta^{33}S$ and $\Delta^{36}S$ values in tropospheric sulfates directly originate from coal itself.

Slight differences in MDF exponents of varying SO_2 oxidation processes could accommodate small variations of $\Delta^{33}S$ in tropospheric SO_2-derived sulfates (±0.1‰) (10) but cannot account for the relatively large nonzero $\Delta^{33}S$ and $\Delta^{36}S$ values in most atmospheric sulfates (including the data in this study) ($-0.66‰ < \Delta^{33}S < 0.53‰$; $-1.6‰ < \Delta^{36}S < -0.1‰$) (Fig. 1). In fact, the seasonal variation of $\Delta^{33}S$ values observed in this study (*SI Appendix*, Fig. S2) does not match the model calculation that only considers MDF processes (10). Additionally, the statistically insignificant ($P > 0.05$) correlation between $\Delta^{33}S$, $\Delta^{36}S$, and $\Delta^{17}O$ [$= \delta^{17}O - 0.52 \times \delta^{18}O$, an isotopic fingerprinting quantifying the relative contribution of SO_2 oxidation processes (3)] shown in this study (*SI Appendix*, Table S1) and by Romero and Thiemens (11) also supports our argument. Replicate analysis and interlaboratory comparisons for the same atmospheric samples in this work demonstrate that the observed nonzero $\Delta^{33}S$ and $\Delta^{36}S$ values are independently reproducible and in agreement (*Materials and Methods*), and the isotopic differences between SO_2 and sulfate therefore further confirm that the nonzero $\Delta^{33}S$ and $\Delta^{36}S$ values in tropospheric sulfates are attributed to photolytic oxidation in the stratosphere or unknown S-MIF processes in the troposphere which require identification.

Altitude-Dependent $\Delta^{33}S$ in the Modern Atmosphere

We observe that $\Delta^{33}S$ is correlated with ^{35}S specific activity (^{35}S-SA) (Fig. 2 and *SI Appendix*, Fig. S2 and Table S1). The relationship between ^{35}S-SA and $\Delta^{33}S$ is best described by a log-linear function in this study, likely reflecting that their vertical profiles in the atmosphere are not exactly the same because of the complex nature of sulfur chemistry and different production processes of ^{35}S (19) and $\Delta^{33}S$ (16) at high altitudes. The age difference of air mass originating from the same altitude (i.e., decayed ^{35}S but the same $\Delta^{33}S$) may also lead to the complex relationship but would not affect our major finding (i.e., positive relationship between ^{35}S and $\Delta^{33}S$) because the decay lifetime of ^{35}S (∼126 d) is significantly longer than the sulfate lifetime in the troposphere (days to weeks). Before this study, radioactive and multiple stable sulfur isotopes in sulfate aerosols were only simultaneously measured by Romero and Thiemens (11) in two samples collected from White Mountain in California. The sample possessing a greater ^{35}S-SA in their pilot study displays a heavier $\Delta^{33}S$ (0.16‰) than the other (0.10‰), consistent with our higher-sensitivity ^{35}S measurements (17, 18).

An extremely low ratio of ^{35}S in coarse to fine particles (0.04) supports the premise that sulfates collected in our remote mountain site were mainly affected by long-range horizontal and vertical transport (*SI Appendix*, *SI Text*). The altitude-dependent variation of $\Delta^{33}S$ revealed by enrichment of stratospherically sourced ^{35}S indicates that sulfate aerosols originating from the higher atmosphere possess a greater $\Delta^{33}S$ value than the boundary layer. Ion-induced binary nucleation of H_2SO_4 and H_2O by galactic cosmic rays was recently identified as a previously ignored process of new particle formations in the free troposphere (23). This process was subsequently found to be mass-dependent in laboratory experiments (24), and therefore it could not explain the ^{35}S-$\Delta^{33}S$ relation observed in this study. We do not rule out the possibility that there is an unknown SO_2 oxidation mechanism which mass-independently enriches ^{33}S in sulfate products in the free troposphere, but, at present, there is no evidence for the existence of such a process. Consequently, we favor the explanation by which downward transport of stratospheric sulfates is the most plausible source of positive $\Delta^{33}S$ values in tropospheric sulfates (11–15).

Romero and Thiemens (11) first measured quadruple sulfur isotopes in tropospheric sulfate aerosols and noted that $\Delta^{33}S$ in the stratosphere might be larger than traditionally thought. Our first-order estimation of $\Delta^{33}S$ values in stratospheric sulfates at East Asia (>4‰) agrees with previous interpretations, although the value should not be viewed as a precise estimate since the relationship between ^{35}S and $\Delta^{33}S$ is nonlinear and complex (see *SI Appendix*, *SI Text* for details). Given large positive $\Delta^{33}S$ values in sulfate products (and negative $\Delta^{33}S$ values in residual SO_2) in SO_2 photolytic oxidation (in the presence of O_2) (25) and

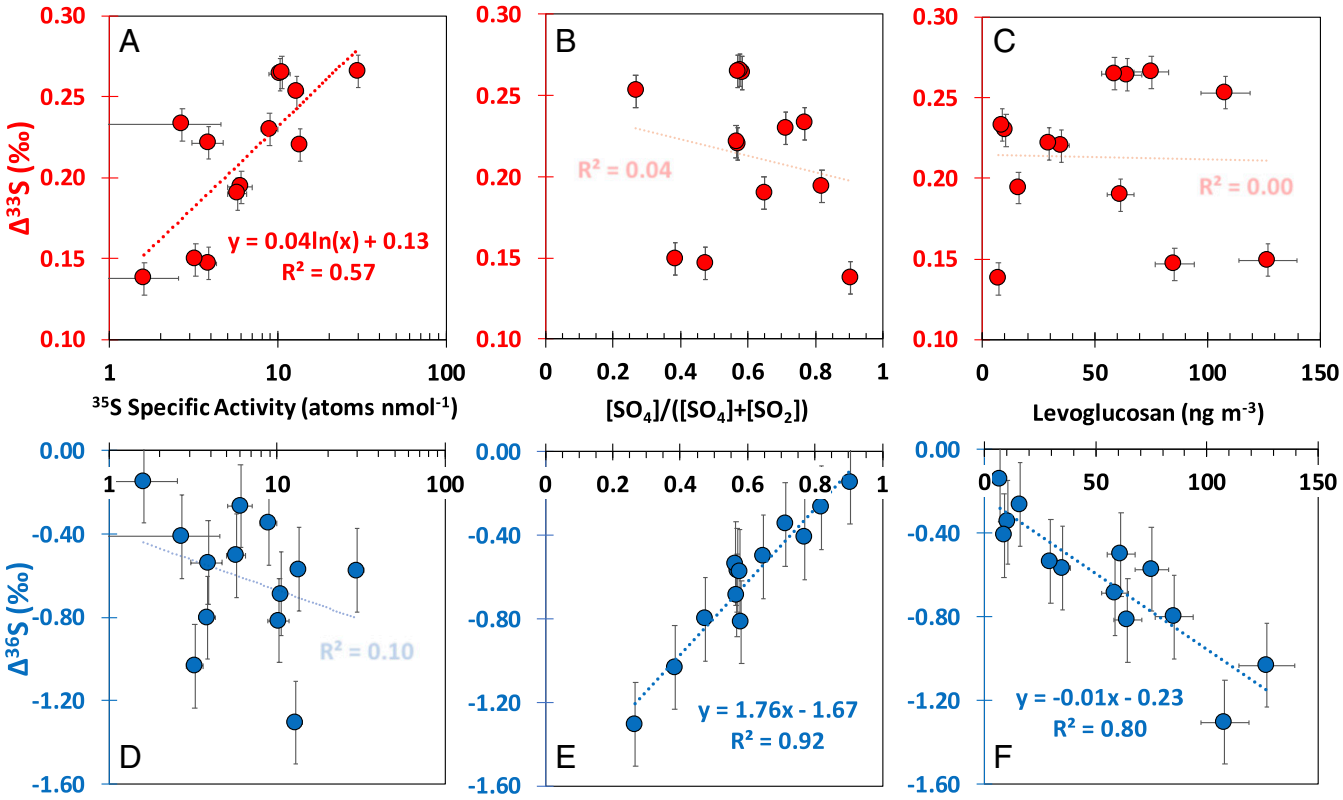

Fig. 2. Scatter plots of S-MIF signatures versus stratospheric and combustion tracers. (*A*–*C*) $\Delta^{33}S$ versus (*A*) ^{35}S specific activity, (*B*) SOR, and (*C*) levoglucosan concentrations. (*D*–*F*) $\Delta^{36}S$ versus (*D*) ^{35}S specific activity, (*E*) SOR, and (*F*) levoglucosan concentrations. Error bars represent 1 SD. If the Pearson correlation is significant at the 0.01 level (*SI Appendix*, Table S1), regression lines, equations, and coefficients of determination (R^2) are shown in darker colors.

frequent downward transport of stratospheric air at midlatitudes (19), it is plausible, and cannot be ruled out, that $\Delta^{33}S$ values (<2‰) of stratospheric sulfates deposited in polar regions (a terminus in poleward transport from the tropics) are much smaller than stratospheric sulfates entrained downward at midlatitudes (where most of atmospheric sulfate measurements were made) as a result of Rayleigh fractionation of $\Delta^{33}S$ during poleward transport. This view is consistent with results from a 2D dynamical/chemical model (26), although a different mechanism was used in that model (SO_3 photolysis, in which the SO_2 acquires positive $\Delta^{33}S$ values), leading to an opposite trend. If this is true, the negative $\Delta^{33}S$ in sulfates deposited in the South Pole during volcanically quiescence times (16) (Fig. 3) may be explained. This hypothesis is also consistent with the decrease of $\Delta^{33}S$ from positive to negative values found in cryospheric records during stratospheric volcano events (8), because more stratospheric SO_2 and sulfates can be transported to the polar regions during stratospheric volcano eruption than during volcanically quiescence times. Additionally, given the high temporal sulfur isotopic heterogeneity (8), it is not impossible that magnitudes of stratospheric S-MIF signatures preserved in the polar regions, even for snow pit samples (time scale: months), were smaller than atmospheric samples (time scale: days).

As argued above, the stratospheric origin of nonzero $\Delta^{33}S$ values observed in most sulfate aerosols in East China and California (Fig. 1) may be therefore dynamically explained by a combination of (*i*) the Asian monsoon anticyclone that efficiently transports SO_2 to the lower stratosphere (27), (*ii*) the sulfate-enriched Asian Tropopause Aerosol Layer in the upper troposphere and lower stratosphere (28), and (*iii*) frequent, active, and intense stratospheric intrusions at midlatitudes of the Northern Hemisphere (19). Our findings therefore highlight the need for further simultaneous measurements (especially by aircraft or balloon collections) and 3D modeling of all five isotopes of sulfur in the modern atmosphere at varying geographic locales to understand the temporal and spatial sulfur isotopic heterogeneity, chemical transformation of sulfur-bearing species during transport, and their implication for tropospheric sulfur budget in the modern atmosphere.

Combustion-Associated $\Delta^{36}S$ in the Modern Atmosphere

The most striking feature in the new data is that, unlike $\Delta^{33}S$, $\Delta^{36}S$ is not clearly correlated with ^{35}S-SA (Fig. 2 and *SI Appendix*, Fig. S2 and Table S1). The poor correlation ($r = -0.18$, $P = 0.55$) indicates that an additional process, apart from SO_2 photochemistry (4), is required to fully explain S-MIF seen in atmospheric sulfates. The sulfur oxidation ratio (SOR) is conventionally expressed as the molar ratio of sulfate to total sulfur (sulfate and SO_2) to quantify the degree of SO_2 oxidation (i.e., formation of secondary sulfate). A low SOR therefore indicates less secondary sulfates (i.e., a relatively large fraction of primary sulfates) in total sulfates. The excellent correlation ($r = 0.96$, $P < 0.000001$) between SOR and $\Delta^{36}S$ (Fig. 2) suggests that $\Delta^{36}S$ is likely linked to the formation of primary sulfate during fossil fuel and/or biomass combustion, with the most negative $\Delta^{36}S$ at low SOR. The *y* intercept (−1.7‰), representing $\Delta^{36}S$ in sulfates near the emission source (characterized by a near-zero SOR as a result of large amounts of SO_2), is close to the most negative $\Delta^{36}S$ (−1.9‰) in primary sulfate aerosols emitted from biomass and diesel combustion (29) (Fig. 1). Alternatively, if the SOR equals 1, the $\Delta^{36}S$ value in tropospheric secondary sulfate (0.1‰) is obtained, which matches SO_2 observations (Fig. 1). This quantitative agreement therefore supports the hypothesis that the large ^{36}S anomaly is associated with combustion processes rather than

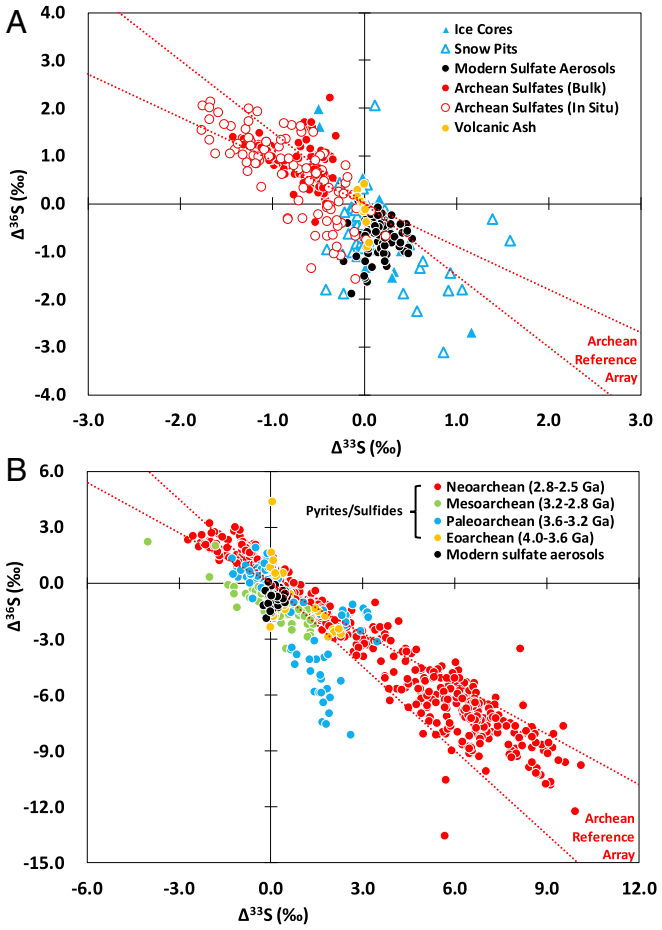

Fig. 3. Similarity of S-MIF signatures in modern atmospheric sulfates and geological records. (*A*) Sulfates from modern aerosols (including the data in this study), ice cores and snow pits, Archean sediments (barites), and volcanic ash. (*B*) Pyrites (FeS_2) and sulfides from different eras in Archean. The red dotted line represents the Archean Reference Array (with slopes of −0.9 and −1.5). See *SI Appendix*, Fig. S4 for the full list of references used for this compilation.

tropospheric SO_2 oxidation. Another independent verifying observation is that there are significant correlations between $\Delta^{36}S$ and various biomass burning tracers (levoglucosan, mannoson, and potassium) (30) in the same samples (Fig. 2 and *SI Appendix*, Table S1).

Our five-sulfur-isotope observation points to a previously underappreciated nonphotochemical channel for producing S-MIF (i.e., fossil fuel and/or biomass combustion). Recent theoretical studies suggested that S-MIF can occur in recombination reactions of elemental sulfur [e.g., $S + S_2 + M \rightarrow S_3 + M$, an analogy of O_3 formation that produces oxygen MIF (3)] as a result of the symmetry effect (31, 32). Although the derived values should be quantitatively validated by laboratory experiments, the theoretical studies (31, 32) reemphasize the potential role of the symmetry effect in S-MIF, which has been noted since early studies (33) but was generally not considered in SO_2 photolytic reactions, because of the trace amount of gaseous S_2, S_3, and S_4 at ambient temperatures (34) and the difficulty of experimental investigation (31, 32). We argue that the elemental sulfur recombination reaction is strictly a thermal reaction, because elemental sulfur vapor (vapor pressure at 717.8 K: 1 atm) contains sulfur allotropes with two to eight sulfur atoms (35). In combustion processes, both S and S_2 are important short-lived intermediates (36). There are a host of potentially relevant reactions (e.g., $SH + S \rightarrow S_2 + H$) (36) that may be crucial in producing these small sulfur allotropes in gas phase, and the high molecular number density may facilitate elemental sulfur recombination reactions. We noted that large S-MIF would be emitted as primary sulfates ($\Delta^{36}S = -1.9‰$) in smoldering combustion (Fig. 1) (29). Because of relatively low O_2 levels in this slow and persistent (up to years) type of combustion rather than flaming fires (37, 38), the fast oxidation reactions (e.g., $SH + O_2 \rightarrow SO + OH$, $SO + O_2 \rightarrow SO_2 + O$) (36) may be slightly restricted, and the above-discussed elemental sulfur related reactions may therefore become important. The potential role of such reactions in producing S-MIF signatures is highlighted and discussed by a recent study focusing on slightly negative $\Delta^{33}S$ values observed in the 19th century, a period with extensive and persistent global biomass burning (15). Our observation provides an additional dimension ($\Delta^{36}S$) to verify the combustion-associated S-MIF signature and to delineate its chemical physics. Given the complexity of combustion processes, a clearly defined $\Delta^{33}S$–$\Delta^{36}S$ relationship was not found in the early combustion experiment (29). The hypothesis proposed here and the corresponding $\Delta^{33}S$–$\Delta^{36}S$ relationship could be tested experimentally in the future to detail all parameters and mechanisms.

Significant correlations with SOR or biomass burning tracers are not observed with respect to $\Delta^{33}S$ (Fig. 2 and *SI Appendix*, Table S1), indicating that $\Delta^{33}S$ is less influenced by combustion processes than is $\Delta^{36}S$. Alternatively, the slightly negative $\Delta^{33}S$ values of primary sulfates emitted from combustion processes (13, 15, 29) (Fig. 1) may be masked by the apparent stratospheric signal (notably positive $\Delta^{33}S$ values) because our samples were collected in a midlatitude remote mountain site. Using the *y* intercepts of $\Delta^{33}S/^{35}S$-SA and $\Delta^{36}S$/levoglucosan fitted curves in Fig. 2 ($\Delta^{33}S = 0.13 \pm 0.02‰$, $\Delta^{36}S = -0.23 \pm 0.07‰$, respectively), we estimate the $\Delta^{36}S/\Delta^{33}S$ ratio of background tropospheric sulfates at East Asia to be -1.8 ± 0.6, a value matching tropospheric sulfates directly observed in a background station at the pristine Tibetan Plateau (-1.8 ± 0.9, $n = 6$) (15) and stratospheric sulfates estimated from Plinian volcanic eruption (-1.9 ± 0.6, $n = 13$) (8) and biomass burning (-1.9 ± 0.1, $n = 3$) (16) records in polar regions (*SI Appendix*, Fig. S3). The consistency may imply the presence of a steady-state stratospheric component in the background troposphere of midlatitudes in the Northern Hemisphere as recently suggested by a decadal observation of stratospherically sourced $\Delta^{17}O$ in tropospheric CO_2 (39).

On the basis of our new five-sulfur-isotope measurements, we identify an altitude-dependent process producing a gradual $\Delta^{36}S/\Delta^{33}S$ slope and a combustion-related process producing a steep slope. The finding explains why inland California, a region more affected by the stratospheric air (19), possesses slightly higher $\Delta^{33}S$ ($0.20 \pm 0.15‰$, $n = 22$) and much smaller $\Delta^{36}S$ ($-0.4 \pm 0.2‰$, $n = 22$) values than the more polluted coastal California ($\Delta^{33}S = 0.16 \pm 0.14‰$, $\Delta^{36}S = -1.0 \pm 0.4‰$, $n = 17$) (11) (Fig. 1). These two MIF end-members, together with the MDF end-member [e.g., tropospheric secondary sulfates (10)], resolve a 15-y-old mystery: the "decoupled" relationship between $\Delta^{33}S$ and $\Delta^{36}S$ in atmospheric sulfates (11) (Fig. 1). The unique isotopic fingerprinting discovered in this study has the potential to quantify the contribution of previously underappreciated sources of sulfates to the present-day troposphere (e.g., stratospheric sulfate, biomass burning, and incomplete residential coal combustion) (13, 15, 16, 40, 41) and their subsequent influences on public health and climate.

Implications for the Understanding of the Archean S-MIF Record

The variability of $\Delta^{36}S/\Delta^{33}S$ slopes in Archean sediments may be an indicator of a changing sulfur cycle on Earth during the appearance and evolution of early life (1, 2, 42), but fundamental chemistry reactions and corresponding biogeochemical processes remain elusive (42, 43). Because laboratory photolysis experiments showed that the $\Delta^{36}S/\Delta^{33}S$ slope is sensitive to the wavelength (*SI Appendix*, Fig. S3), experimental and modeling efforts have been

focused on tuning atmospheric composition to reproduce the observed Archean array (44, 45). However, thermochemical sulfate reduction was proposed as an alternative or additional S-MIF mechanism to explain the Archean record (46), but this process was attributed to magnetic isotope effects (47), which only lead to ^{33}S anomalies and contrast with observations in nature such as Archean rocks, ice cores, and present-day aerosols (Fig. 3). By comparison of sulfur isotopic signatures between modern and Archean record, recent studies suggest that varying atmospheric S-MIF processes (photolytic reactions of SO_2/OCS, and possibly recombination reactions of elemental sulfur) may have operated in both periods (15, 16, 48).

Our field-based observation has shown that, certainly for today, the isotopic anomalies in ^{33}S and ^{36}S appear decoupled in the measured natural samples, and their corresponding photochemical and nonphotochemical processes can be identified by simultaneous measurements of radiosulfur and combustion indices. The fitted $\Delta^{36}S/\Delta^{33}S$ slope (-4.0 ± 1.0) in our selected aerosol samples (without samples strongly affected by combustion; see *SI Appendix, SI Text* and Fig. S2) is compatible with the relatively steep $\Delta^{36}S/\Delta^{33}S$ slope of -3.6 ± 1.8 observed in some Paleoarchean [3.6 Ga to 3.2 Ga, an era characterized by intense volcanic activity (49)] pyrites (50) (Fig. 3), indicating that photochemical and nonphotochemical S-MIF processes may have concomitantly occurred in primitive Earth. In the Archean, it is widely accepted that S-MIF signatures are from photochemical reactions of sulfur-bearing species emitted from volcanoes, and therefore volcanic activity is required in all Archean S-MIF models (1, 43). Venting and polymerization of gaseous S_2 is ubiquitous on Io (one of Galilean moons), the most volcanically active body in the solar system (51). At terrestrial volcanic vents and fumaroles, elemental sulfur deposits formed in high-temperature sulfur-bearing gases are commonly found (35, 52). Therefore, it is likely that basic reactions responsible for nonphotochemical S-MIF processes in combustion [probably recombination reactions (31, 32)], which are characterized by large ^{36}S anomalies, may occur in terrestrial volcanoes throughout Earth's history.

Existing data show a negative $\Delta^{36}S$ value ($-0.9‰$) and a near-zero $\Delta^{33}S$ value ($0.03‰$) in modern volcanogenic sulfate aerosols at the point of emission (53) (Fig. 3). This S-MIF signature, similar to combustion-associated $\Delta^{36}S$ observed in this field-based study and previous chamber experiments (29), likely resulted from thermochemical S-MIF processes as suggested previously, as a photochemical source is not possible. Steep $\Delta^{36}S/\Delta^{33}S$ slopes are also observed in sulfates leached from Quaternary volcanic ash (54), and in some igneous rocks from the Eoarchean (4.0 Ga to 3.6 Ga), an era during which Earth might be intensively impacted by asteroid storm (the Late Heavy Bombardment) (55) (Fig. 3). These similarities emphasize the need for further sulfur isotopic measurements of present-day volcanic gases and solids formed in the gas phase to understand sulfur isotope partitioning in these thermal reactions and its implications for early Earth evolution. Given that both SO_2 photolysis and elemental sulfur polymerization are relevant to Archean volcanism, the Archean ^{33}S and ^{36}S anomalies could, in fact, come from the same volcanoes but different reactions, which lead to varying $\Delta^{36}S/\Delta^{33}S$ slopes in the Archean record (Fig. 3). These two distinct S-MIF processes and their interplay are not concomitantly explored in the past. The present data suggest that, with extended experimental and modeling efforts on providing the new chemical physics of S-MIF in elemental sulfur recombination reactions, the Archean S-MIF record and its implications for the atmospheric, oceanic, and microbial processes on primitive Earth may potentially yield deeper insight in the future.

Materials and Methods

Aerosol, SO_2, and coal samples were collected at a background mountain site in East Asia, a Chinese megacity (during the coal-burning season), and three coal mines across China, respectively (*SI Appendix*, Fig. S1). Eight isotopes (^{32}S, ^{33}S, ^{34}S, ^{35}S, ^{36}S, ^{16}O, ^{17}O, and ^{18}O) in sulfate aerosols and quadruple stable sulfur isotopes (^{32}S, ^{33}S, ^{34}S, and ^{36}S) in SO_2 and coal samples were measured. High-sensitivity radioactive sulfur isotope (cosmogenic ^{35}S) measurements were conducted at University of California, San Diego using an ultra-low-level liquid scintillation spectrometer (Wallac 1220 Quantulus) technique (17, 18). Quadruple stable sulfur isotopes (^{32}S, ^{33}S, ^{34}S, and ^{36}S) were measured in two independent laboratories (University of California, San Diego and University of Science and Technology of China) using different fluorination methods and isotope ratio mass spectrometers (IRMS) (Thermo Finnigan MAT 253), and were reported in isotope ratios defined as $\delta^{3x}S = (^{3x}S/^{32}S)_{sample}/(^{3x}S/^{32}S)_{VCDT} - 1$, where x = 3, 4, and 6 and VCDT stands for the Vienna Canyon Diablo Troilite reference material. It is assumed that the International Atomic Energy Agency (IAEA) S1 has a sulfur isotopic composition on the VCDT scale of $\delta^{34}S = -0.3‰$, $\Delta^{33}S = 0.10‰$, and $\Delta^{36}S = -0.80‰$ (56). The IAEA S1 standard was routinely fluorinated and measured during the study period, and our values match the above-mentioned values and those obtained from another independent laboratory (University of Maryland) (57). Overall uncertainties (1 SD) of $\delta^{34}S$, $\Delta^{33}S$, and $\Delta^{36}S$ in fluorination and isotopic measurements at both laboratories are less than 0.2‰, 0.01‰, and 0.2‰, respectively. Samples with sufficient sulfur and laboratory Ag_2S standards were replicated for full chemistry (reduction, fluorination, and isotopic measurements) in both laboratories for comparing the measured $\Delta^{33}S$ and $\Delta^{36}S$ values. Differences between two laboratories and replicated experiments are within the reported analytical uncertainties (*SI Appendix*, Tables S2 and S3). The high reproducibility of $\Delta^{33}S$ and $\Delta^{36}S$ for the same atmospheric sample in independent laboratories allows us to assure that the measured S-MIF signatures were not an experimental artifact resulting from any unknown S-MIF fractionation process due to the chemically complex matrix in the atmospheric samples. Triple stable oxygen isotopes (^{16}O, ^{17}O, and ^{18}O) were measured at University of California, San Diego using a pyrolysis method (58) and an IRMS. Assuming the molar ratio of sulfate to sodium (a sea salt tracer) to be 0.0604 in sea salt spray, we estimated the sea salt content in each fine sulfate sample to be less than 1.5% (with an average of $0.9 \pm 0.3\%$) (20). Therefore, all isotopic compositions reported in this study are not corrected for non–sea-salt sulfates. Concentrations of water-soluble ions (Na^+, NH_4^+, K^+, Ca^{2+}, Mg^{2+}, Cl^-, NO_3^-, and SO_4^{2-}), saccharidic tracers for biomass burning (levoglucosan and mannosan), and carbonaceous species in the same aerosol samples were determined using two ion chromatographies (Dionex ICS-1600 and ICS-2100), a high-performance anion exchange chromatography with pulsed amperometric detection (Dionex ICS-3000) technique (30), and a Desert Research Institute aerosol carbon analyzer (model 2001; Atmoslytic Inc.) (59), respectively. Detailed sampling and analytical procedures can be found in *SI Appendix, SI Text*. All sulfur isotope data and relevant stratospheric/combustion tracer data reported in this study are presented in *SI Appendix*, Tables S2–S5.

ACKNOWLEDGMENTS. We appreciate T. Jackson's technical advice and guidance in stable isotope analysis, K. Chen's and X. Huang's assistance in stable sulfur isotopic analysis and compiling Archean data, R. Zhang's assistance in the fieldwork, and the reviewers for their insightful comments that led us to an improvement of this work. M. Lin acknowledges a fellowship from the Guangzhou Elite Project (Award JY201303) and the 2017 Chinese Government Award for Outstanding Self-Financed Students Abroad. This study was partially supported by the National Natural Science Foundation of China (Grants 41330102, 41520104007, 41721002, 41475119, and 41603119), the 111 Project, and Chinese Academy of Sciences (Grant QYZDY-SSW-DQC031).

1. Lyons TW, Reinhard CT, Planavsky NJ (2014) The rise of oxygen in Earth's early ocean and atmosphere. *Nature* 506:307–315.
2. Farquhar J, Bao H, Thiemens M (2000) Atmospheric influence of Earth's earliest sulfur cycle. *Science* 289:756–759.
3. Thiemens MH (2006) History and applications of mass-independent isotope effects. *Annu Rev Earth Planet Sci* 34:217–262.
4. Ono S (2017) Photochemistry of sulfur dioxide and the origin of mass-independent isotope fractionation in Earth's atmosphere. *Annu Rev Earth Planet Sci* 45:301–329.
5. Franz HB, et al. (2014) Isotopic links between atmospheric chemistry and the deep sulphur cycle on Mars. *Nature* 508:364–368.
6. Chakraborty S, Jackson TL, Ahmed M, Thiemens MH (2013) Sulfur isotopic fractionation in vacuum UV photodissociation of hydrogen sulfide and its potential relevance to meteorite analysis. *Proc Natl Acad Sci USA* 110:17650–17655.
7. Savarino J, Romero A, Cole-Dai J, Bekki S, Thiemens MH (2003) UV induced mass-independent sulfur isotope fractionation in stratospheric volcanic sulfate. *Geophys Res Lett*, 30:2131.

8. Baroni M, Thiemens MH, Delmas RJ, Savarino J (2007) Mass-independent sulfur isotopic compositions in stratospheric volcanic eruptions. *Science* 315:84–87.
9. Martin E, Bindeman I (2009) Mass-independent isotopic signatures of volcanic sulfate from three supereruption ash deposits in Lake Tecopa, California. *Earth Planet Sci Lett* 282:102–114.
10. Harris E, Sinha B, Hoppe P, Ono S (2013) High-precision measurements of ^{33}S and ^{34}S fractionation during SO_2 oxidation reveal causes of seasonality in SO_2 and sulfate isotopic composition. *Environ Sci Technol* 47:12174–12183.
11. Romero AB, Thiemens MH (2003) Mass-independent sulfur isotopic compositions in present-day sulfate aerosols. *J Geophys Res Atmos,* 108:4524.
12. Guo ZB, et al. (2010) Identification of sources and formation processes of atmospheric sulfate by sulfur isotope and scanning electron microscope measurements. *J Geophys Res Atmos,* 115:D00K07.
13. Han X, et al. (2017) Multiple sulfur isotope constraints on sources and formation processes of sulfate in Beijing $PM_{2.5}$ aerosol. *Environ Sci Technol* 51:7794–7803.
14. Kim Y, et al. (2018) The origin and migration of the dissolved sulfate from precipitation in Seoul, Korea. *Environ Pollut* 237:878–886.
15. Lin M, et al. (2018) Atmospheric sulfur isotopic anomalies recorded at Mt. Everest across the Anthropocene. *Proc Natl Acad Sci USA* 115:6964–6969.
16. Shaheen R, et al. (2014) Large sulfur-isotope anomaly in nonvolcanic sulfate aerosol and its implications for the Archean atmosphere. *Proc Natl Acad Sci USA* 111: 11979–11983.
17. Brothers LA, et al. (2010) Optimized low-level liquid scintillation spectroscopy of 35S for atmospheric and biogeochemical chemistry applications. *Proc Natl Acad Sci USA* 107:5311–5316.
18. Lin M, Thiemens MH (2018) Accurate quantification of radiosulfur in chemically complex atmospheric samples. *Anal Chem* 90:2884–2890.
19. Lin M, Su L, Shaheen R, Fung JCH, Thiemens MH (2016) Detection of deep stratospheric intrusions by cosmogenic 35S. *Proc Natl Acad Sci USA* 113:11131–11136.
20. Lin M, et al. (2017) Vertically uniform formation pathways of tropospheric sulfate aerosols in East China detected from triple stable oxygen and radiogenic sulfur isotopes. *Geophys Res Lett* 44:5187–5196.
21. Su S, Li B, Cui S, Tao S (2011) Sulfur dioxide emissions from combustion in China: From 1990 to 2007. *Environ Sci Technol* 45:8403–8410.
22. Dai SF, et al. (2012) Geochemistry of trace elements in Chinese coals: A review of abundances, genetic types, impacts on human health, and industrial utilization. *Int J Coal Geol* 94:3–21.
23. Kirkby J, et al. (2011) Role of sulphuric acid, ammonia and galactic cosmic rays in atmospheric aerosol nucleation. *Nature* 476:429–433.
24. Enghoff MB, et al. (2012) An isotopic analysis of ionising radiation as a source of sulphuric acid. *Atmos Chem Phys* 12:5319–5327.
25. Whitehill AR, Jiang B, Guo H, Ono S (2015) SO_2 photolysis as a source for sulfur mass-independent isotope signatures in stratospehric aerosols. *Atmos Chem Phys* 15: 1843–1864.
26. Pavlov AA, Mills MJ, Toon OB (2005) Mystery of the volcanic mass-independent sulfur isotope fractionation signature in the Antarctic ice core. *Geophys Res Lett* 32:L12816.
27. Bourassa AE, et al. (2012) Large volcanic aerosol load in the stratosphere linked to Asian monsoon transport. *Science* 337:78–81.
28. Yu P, Toon OB, Neely RR, Martinsson BG, Brenninkmeijer CAM (2015) Composition and physical properties of the Asian tropopause aerosol layer and the North American tropospheric aerosol layer. *Geophys Res Lett* 42:2540–2546.
29. Lee CCW, Savarino J, Cachier H, Thiemens MH (2002) Sulfur (S-32, S-33, S-34, S-36) and oxygen (O-16, O-17, O-18) isotopic ratios of primary sulfate produced from combustion processes. *Tellus B Chem Phys Meterol* 54:193–200.
30. Engling G, et al. (2006) Determination of levoglucosan in biomass combustion aerosol by high-performance anion-exchange chromatography with pulsed amperometric detection. *Atmos Environ* 40:S299–S311.
31. Babikov D (2017) Recombination reactions as a possible mechanism of mass-independent fractionation of sulfur isotopes in the Archean atmosphere of Earth. *Proc Natl Acad Sci USA* 114:3062–3067.
32. Babikov D, Semenov A, Teplukhin A (2017) One possible source of mass-independent fractionation of sulfur isotopes in the Archean atmosphere of Earth. *Geochim Cosmochim Acta* 204:388–406.
33. Bainssahota SK, Thiemens MH (1989) A mass-independent sulfur isotope effect in the nonthermal formation of S2F10. *J Chem Phys* 90:6099–6109.
34. Lyons JR (2007) Mass-independent fractionation of sulfur isotopes by isotope-selective photodissociation of SO_2. *Geophys Res Lett* 34:L22811.
35. Kumar M, Francisco JS (2017) Elemental sulfur aerosol-forming mechanism. *Proc Natl Acad Sci USA* 114:864–869.
36. Gardiner WC (2000) *Gas-Phase Combustion Chemistry* (Springer, New York).
37. Rein G (2009) Smouldering combustion phenomena in science and technology. *Int Rev Chem Eng* 1:3–18.
38. Belcher CM, Yearsley JM, Hadden RM, McElwain JC, Rein G (2010) Baseline intrinsic flammability of Earth's ecosystems estimated from paleoatmospheric oxygen over the past 350 million years. *Proc Natl Acad Sci USA* 107:22448–22453.
39. Thiemens MH, Chakraborty S, Jackson TL (2014) Decadal $\Delta^{17}O$ record of tropospheric CO_2: Verification of a stratospheric component in the troposphere. *J Geophys Res Atmos* 119:6221–6229.
40. Du QQ, et al. (2016) An important missing source of atmospheric carbonyl sulfide: Domestic coal combustion. *Geophys Res Lett* 43:8720–8727.
41. Yan C, et al. (2018) Residential coal combustion as a source of levoglucosan in China. *Environ Sci Technol* 52:1665–1674.
42. Farquhar J, et al. (2007) Isotopic evidence for Mesoarchaean anoxia and changing atmospheric sulphur chemistry. *Nature* 449:706–709.
43. Halevy I, Johnston DT, Schrag DP (2010) Explaining the structure of the Archean mass-independent sulfur isotope record. *Science* 329:204–207.
44. Endo Y, Ueno Y, Aoyama S, Danielache SO (2016) Sulfur isotope fractionation by broadband UV radiation to optically thin SO_2 under reducing atmosphere. *Earth Planet Sci Lett* 453:9–22.
45. Ueno Y, et al. (2009) Geological sulfur isotopes indicate elevated OCS in the Archean atmosphere, solving faint young sun paradox. *Proc Natl Acad Sci USA* 106: 14784–14789.
46. Watanabe Y, Farquhar J, Ohmoto H (2009) Anomalous fractionations of sulfur isotopes during thermochemical sulfate reduction. *Science* 324:370–373.
47. Oduro H, et al. (2011) Evidence of magnetic isotope effects during thermochemical sulfate reduction. *Proc Natl Acad Sci USA* 108:17635–17638.
48. Muller É, Philippot P, Rollion-Bard C, Cartigny P (2016) Multiple sulfur-isotope signatures in Archean sulfates and their implications for the chemistry and dynamics of the early atmosphere. *Proc Natl Acad Sci USA* 113:7432–7437.
49. Philippot P, van Zuilen M, Rollion-Bard C (2012) Variations in atmospheric sulphur chemistry on early Earth linked to volcanic activity. *Nat Geosci* 5:668–674.
50. Wacey D, Noffke N, Cliff J, Barley ME, Farquhar J (2015) Micro-scale quadruple sulfur isotope analysis of pyrite from the similar to 3480 Ma Dresser Formation: New insights into sulfur cycling on the early Earth. *Precambrian Res* 258:24–35.
51. Spencer JR, Jessup KL, McGrath MA, Ballester GE, Yelle R (2000) Discovery of gaseous S2 in Io's Pele plume. *Science* 288:1208–1210.
52. Taran YA, Pilipenko VP, Rozhkov AM, Vakin EA (1992) A Geochemical model for fumaroles of the Mutnovsky volcano, Kamchatka, Ussr. *J Volcanol Geotherm Res* 49: 269–283.
53. Mather TA, et al. (2006) Oxygen and sulfur isotopic composition of volcanic sulfate aerosol at the point of emission. *J Geophys Res Atmos* 111:D18205.
54. Bindeman IN, Eiler JM, Wing BA, Farquhar J (2007) Rare sulfur and triple oxygen isotope geochemistry of volcanogenic sulfate aerosols. *Geochim Cosmochim Acta* 71: 2326–2343.
55. Thomassot E, O'Neil J, Francis D, Cartigny P, Wing BA (2015) Atmospheric record in the Hadean Eon from multiple sulfur isotope measurements in Nuvvuagittuq Greenstone Belt (Nunavik, Quebec). *Proc Natl Acad Sci USA* 112:707–712.
56. Ueno Y, Ono S, Rumble D, Maruyama S (2008) Quadruple sulfur isotope analysis of ca. 3.5 Ga Dresser Formation: New evidence for microbial sulfate reduction in the early Archean. *Geochim Cosmochim Acta* 72:5675–5691.
57. Zhang G, et al. (2017) Redox chemistry changes in the Panthalassic Ocean linked to the end-Permian mass extinction and delayed Early Triassic biotic recovery. *Proc Natl Acad Sci USA* 114:1806–1810.
58. Savarino J, Alexander B, Darmohusodo V, Thiemens MH (2001) Sulfur and oxygen isotope analysis of sulfate at micromole levels using a pyrolysis technique in a continuous flow system. *Anal Chem* 73:4457–4462.
59. Cao JJ, et al. (2004) Spatial and seasonal variations of atmospheric organic carbon and elemental carbon in Pearl River Delta Region, China. *Atmos Environ* 38:4447–4456.